Journal of Engineering and Applied Sciences 13 (Special Issue 11): 8675-8677, 2018
ISSN: 1816-949X

Spiral Resonator Bandstop Filter Design with Spurlines

Bhanu Shrestha
Department of Electronic Engineering, Kwangwoon University, 447-1 Wolgye-dong,
Nowon-ku, 139-701 Seoul, Korea

Abstract: In this study, we designed and characterized compact Double Spiral Resonator Bandstop Filter (DSR-BSF) with double spurlines. The double spiral and double spurline were used to enhance its performance with dual mode and to suppress the harmonics respectively. Therefore, the designed DSR-BSF achieves a significantly low insertion loss and wider band rejection characteristics. The operating frequency of the measured DSR-BSF is 3.2 GHz for S-band application with a minimum insertion loss of <42.1 dB and return loss is below 0.03 dB in measurement results. The fractional bandwidth was also achieved approximately 54%. The measurement results have a good agreement with the simulation results. Implementation of such resonator filters in Integrated Passive Device (IPD) technology is also possible due to its compactness. The overall dimension of the developed DS-BSF was 0.95×0.34 λg.

Key words: Double spiral bandstop filter, double spurlines resonator, microstrip BSF, spurline technique, spurline BSF, measurement

INTRODUCTION

Microstrip compact Bandstop Filters (BSFs) are widely used to suppress harmonics and unnecessary signals in the communication system due to low cost and low weight. Many researchers are currently designing microstrip bandstop filters such as a BSF with open-circuited stubs, a BSF with cross-coupling stubs, a square split ring BSF, stepped impedance resonator BSF and a BSF using a square loop resonator to have bandstop characteristics with low insertion loss, deeper rejection and highly integrated patterns (Chiu and Xue, 2012; Mukherjee *et al*., 2012; La *et al*., 2014; Liu *et al*., 2013). However, we can also consider the double spurlines in both input and output port to reduce the harmonics and get good bandstop characteristics with reduction of size. Such configuration can be advantageous to upgrade the device performance in order to implement in the communication system (Luo *et al*., 2010; Shrestha and Kim, 2012; Shrestha *et al*. 2017). Therefore, in this study, we applied double spurlines in each part in the DSR-BSF to achieve a stopband response with good reflection zeros. The spurline configuration can overcome the problems associated with harmonics, miniaturization, ease of fabrication and low material cost relative to other various types of resonators such as hairpin resonators and dielectric resonators.

DSR-BSF design and simulation: A compact dual-mode Double Spiral Resonator Bandstop Filter (DSR-BSF) with double spurlines is designed and simulated using the sonnet EM simulator. The DSR-BSF was built by using double spurlines in the both sides of spiral resonator in series. The BSF was fabricated using a Teflon substrate with a thickness and dielectric constant of 0.54 and 2.54 mm, respectively. A schematic layout of the DS-BSF is depicted in Fig. 1. The double spiral was composed of two single rectangular spiral connected in series as shown in the Fig. 1. In this study, the calculated value of the double spiral length, L_s was 0.203 times the guided wavelength (λ_g). The gap between two spirals and turn spacing were C_G and C_g were optimized to 0.017 and 0.013 times the guided wavelength (λ_g) respectively. The length and width of the whole spurlines were 0.009 λ_g and and 0.006 λ_g, respectively which are responsible for suppressing the harmonics as well as enhancing reflection zero characteristics to have a good device performance. In the same manner, the height of the spirals, h_1 and h_2 were adjusted as 0.074 λ_g each for optimizing the DSR-BSF size and its S-parameter responses. The D represents the distance between spiral resonators and reference lines which were 0.120 λ_g in both sides. The reference lines in both ports were 0.065 λ_g and the width, W of the reference line was 0.146 λ_g and both ports were terminated at 50 Ω.

Figure 2 shows the simulation results of DSR-BSF with double spurline which has a dual mode with the insertion loss (S_{21}) and return loss (S_{11}) of 0.03 dB and 42.1 dB, respectively at the center operating a frequency of 3.2 GHz. At the same time, transmission zero was improved with harmonics too which can be confirmed by the simulation result depicted in Fig. 2. The quality of the reflection zeros demonstrated selective frequency rejection at reflection zero at 5.9 GHz. We can calculate the guided wavelength of the microstrip line used for designing DSR-BSF as Eq. 1:

$$\lambda_g = \frac{\lambda}{\sqrt{\varepsilon_{eff}}} = \frac{c}{f_{bs}\sqrt{\varepsilon_{eff}}} \quad (1)$$

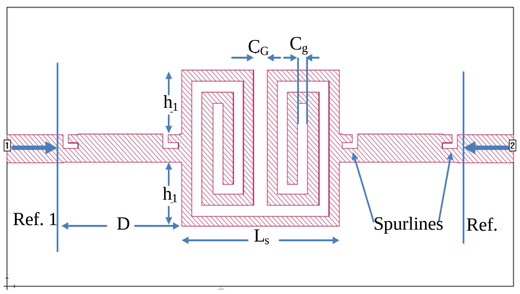

Fig. 1: Schematic of compact and miniaturized double spiral resonator BSF with dual spurlines

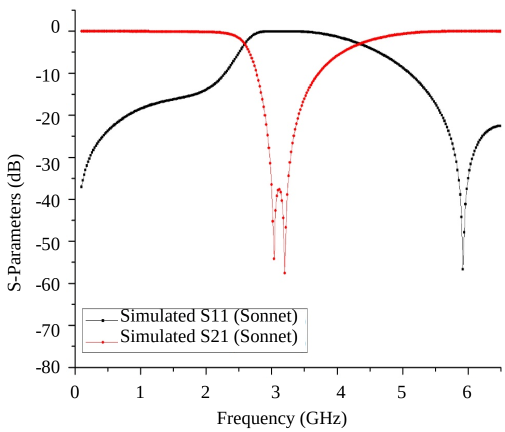

Fig. 2: Simulated frequency responses of the miniaturized BSF

Where:

- L = The length of the spurline
- C = The speed of light (3×10^8 m/sec)
- f_{bs} = The bandstop frequency
- ε_{eff} = The effective permittivity of the substrate (Shrestha and Cho, 2017)

We can calculate the value of guided wavelength using Eq. 1 that results in 30.73 mm.

Equivalent circuits: The equivalent circuit for compact double spiral resonator dual mode DSR-BSF with double spurline which consists of mainly an LC network is shown in Figure 3. In this model, the LC circuit was used to obtain the resonance characteristics. In this case, resistance, R was not considered which was used to evaluate the radiation effect and loss of the device. The resonance frequency of using LC network can be estimated by using the Eq. 2:

$$f_{sb} = 1/(2\pi\sqrt{LC})$$

where, L and C are the total inductance and capacitance respectively. The total capacitance also includes a fringing capacitance.

As illustrated in Fig. 3, the two spiral inductors are represented by L_1 and C_g and these are connected in series can be expressed by L_2. The gap between two spiral resonators can be represented by C_G, however, its effect is much more less than the turning gap (C_g) of spiral, hence, it is shown in dotted line in the equivalent circuit. The double spurlines are embedded in both sides which can also be denoted by LC network. Eventually, we can get the LC network for the whole part of the DSR-BSF. Cp_1 and Cp_2 in the equivalent circuit represent the pad capacitances. The input and output are taken from port 1 and 2, respectively.

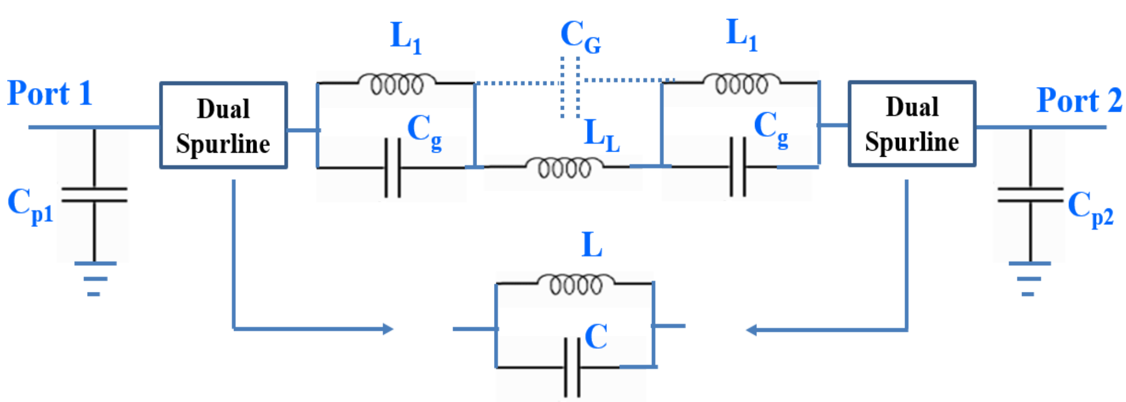

Fig. 3: Equivalent circuit of the miniaturized BSF

Table 1: A summary of the performance of compact DSR-BSF showing comparison of simulated and measured data

Parameters	Simulated results (GHz)	Measured results (GHz)
Frequency	3.2	3.20
Insertion loss (S21)	-42.2	-42.10
Return loss (S11)	0.02	0.03
Bandwidth rejection	1.70	1.73
Size	0.95×0.34 λg	

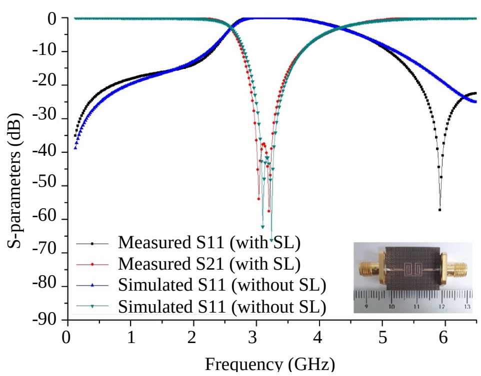

Fig. 4: Measured and simulated frequency responses

RESULTS AND DISCUSSION

The bandstop resonator filter was fabricated on a Teflon substrate with a thickness of 0.54 mm, the dielectric constant of 2.54 and loss tangent of 0.001 using a wet etching process to validate the simulation results performed using Sonnet EM simulator tool. The bandstop filter (BSF) was quite compact and miniaturized, measuring 5.6×20 mm^2 including reference line which was terminated with 50 Ω in input and output ports. The fabricated DSR-BSF was characterized using an Agilent (HP) 8510 C Vector Network Analyzer (VNA). In the measurement, the insertion loss (S_{21}) and return loss (S_{11}) were -42.1 dB and 0.03 dB, respectively were achieved at a resonant frequency of 3.2 GHz. These characteristics of DSR-BSF are very good for practical applications. There was good agreement between the simulation and measurement results due to accurate design considerations which are shown in Fig. 4. The fractional bandwidth of the developed DSR-BSF was measured to be 1.73 GHz which is approximately 54% with wide rejection. Such a BSF can also be implemented in a microstrip oscillator to obtain low-phase-noise characteristics. Furthermore, we can also integrate it using the Integrated Passive Device technology (IPD) after further miniaturization (Table 1).

CONCLUSION

A compact double spiral resonator bandstop filter developed based on the double spurline technique was designed, fabricated and characterized. The double spurline technique was implemented in between the double spiral resonator to obtain good device performance and the transmission coefficients responses with good harmonic suppression characteristics. The characterization data were in good agreement with the simulated results. The DSR-BSF demonstrated a wide and deep rejection bandwidth of approximately 54% which can be applied to the wide band application. This double spurline technique was verified to be suitable also for practical applications in communications systems and feasible for fabrication via. Integrated Passive Device (IPD) technology due to its performance potential and inherently small size.

REFERENCES

Chiu, L. and Q. Xue, 2012. A simple microstrip bandstop filter using cross-coupling stubs. Intl. J. Microwave Sci. Technol., 2012: 1-6.

La, D.S., C.M. Huang, X.Y. Qiu and J.L. Zhang, 2014. Compact gradually variational stepped impedance resonator band-stop filters. Microwave Opt. Technol. Lett., 56: 1-3.

Liu, Y., H.X. Zheng and L.Y. Feng, 2013. A compact dual-mode resonator with square loops and its bandpass filter applications. Prog. Electromagnet. Res., 4: 51-61.

Luo, S., L. Zhu and S. Sun, 2010. A dual-band ring-resonator bandpass filter based on two pairs of degenerate modes. IEEE. Trans. Microwave Theory Tech., 58: 3427-3432.

Mukharjee, S., S. Bhattacharjee, D. Poddar and S.K. Saurabh, 2012. Design of wide band microstrip bandstop filter with open-circuited stubs for wireless communication applications. Intl. J. Electron. Commun. Compd. Technol., 2: 259-261.

Shrestha, B. and N.Y. Kim, 2012. Spurline resonators design and its implementation to microwave oscillators. Microwave Optical Technol. Lett., 54: 171-176.

Shrestha, B., J.H. Yi and S. Cho, 2017. Wideband open stub BPF for cognitive radio system applications. Intl. J. Sens. Networks, 25: 198-205.